IAGA WG 1.2 on Electromagnetic Induction in the Earth
20th Workshop Abstract
Giza, Egypt , September 18-24, 2010

Southern Africa Lithosphere: Comparison of Seismic and Electrical Parameters

Alan G. Jones[1], Stewart Fishwick[2], Rob L. Evans[3]

[1] Dublin Institute for Advanced Studies, Dublin, Ireland
[2] Department of Geology, University of Leicester, Leicester, England
[3] Woods Hole Oceanographic Institution, Woods Hole, MA, USA

SUMMARY
Seismic velocity is primarily a function of bulk properties of the media and electrical resistivity is primarily a function of the properties of a minor phase in the rock matrix (low order partial melt, presence of conducting irons, oxides, water, hydrogen diffusion, etc.), so one might not expect the two to correlate. However, for the Southern African lithosphere there does appear to be a systematic correlation, suggesting that both are primarily functions of temperature variation rather than compositional variation.

Comparisons at various depths of slices from a new high-resolution (1.5 deg) seismic model, derived from surface wave inversion of events along continental paths and of new electrical images from the SAMTEX experiment reveal correlations at both large and small scales. The existence of these correlations, which can be defined quantitatively by a quadratic regression between log(resistivity) and shear wave velocity, indicates that the two are functions of the same parameters, namely temperature, physical state, magnesium number, and composition. This suggests that joint inversion would be worthwhile, where the two datasets should be inverted directly for petrophysical parameters.

Keywords: Lithosphere, petro-physical properties, Southern Africa, SAMTEX

INTRODUCTION

The plate tectonic paradigm is a remarkably successful model describing the Earth's dominant tectonic process. There is much debate, however, concerning how far back this paradigm is a valid model to interpret the cryptic rock record. Some argue that it can be validly applied early in Earth's history (e.g., de Wit 1998), whereas others argue that plate tectonics, sensu *stricto*, is not applicable before ca. 2.5 Byr ago, and that other processes, such as sagduction and mantle plumes, dominated during the Archean era (e.g., Bleeker, 2003; Davies, 1992; Hamilton, 1998; van Kranendonk, 2003). Indeed, some believe that plate tectonics was not establishing until late in the Proterozoic (Stern, 2005; Stern, 2007), although this view is seriously questioned (Hoffman, 2006; Stern, 2006)

Directly coupled with this question is uncertainty of the formation process of Archean-aged cratonic lithosphere. The extant, competing models reveal our limitations in fundamental information of the sub-continental lithospheric mantle (SCLM), a knowledge gap that can be partially addressed through obtaining physical and geometrical information of fossil structures using geophysical imaging. To date this has been undertaken primarily using passive seismology, but over the last decade deep-probing magnetotellurics (MT) has developed and applied for this problem, and demonstrated that MT data, when combined with other geoscientific information, provides significant constraints on formation processes (e.g., Davis et al., 2003; Muller et al., 2009).

Whereas seismic methods primarily are a function of the bulk properties of the media, electrical conductivity is often primarily a function of the properties of a reasonably-well interconnected minor phase in the rock matrix that permits electronic or ionic conduction, such as low order partial melt (ionic), sulphides (electronic), oxides (electronic), graphite/carbon (electronic), saline water (ionic), hydrogen diffusion (ionic), etc. Thus, the two can be complementary when investigation the geometry of the subsurface (Jones, 1998; Jones, 1999b).

However, when the rocks do not contain any well-interconnected minor phase and are "dry", i.e., no proton (H+) diffusion, then conduction of the electric field is by semi-conduction processes in the silicate minerals, such as polaron-hopping (see Yoshino, 2010, for an excellent recent review). Such can be the case for cratonic lithosphere, which represents the simplest rocks on the planet comprising only four minerals in the assemblage; predominantly olivine (Ol) and orthopyroxene (Opx), with minor amounts of clinopyroxene (Cpx) and garnet (Gn), with "exotic" minerals at sub-1% levels so can be ignored.

PHYSICAL PARAMETERS OF MANTLE ROCKS BENEATH SOUTHERN AFRICA

Based on empirical petro-physical equations derived through laboratory experiments, Jones et al. (2009b) proposed an approach to "build" a rock and derive its physical observable parameters, namely bulk and shear moduli, density and conductivity, from the relative proportion of these four minerals, the oxidation state of Ol, the amount of Fe in each mineral (given by the magnesium number, Mg#, which is (1-Fe)*100), and the ambient pressure and temperature. From the moduli and density, seismic velocities (shear, compressional and bulk) can easily be calculated. There are a variety of methods for determining the bulk properties of a rock from its constituent minerals – in seismology the Voigt-Reuss-Hill (Hill, 1952; Reuss, 1929; Voigt, 1928) average is the most often applied approach, whereas in electrical methods a wide variety of approaches have been used. Jones et al. (2009b) chose to take the most conservative approach possible, and determined the extremal bounds of the physical parameters using a Hashin-Shtrikman approach adding consideration for surface effects due to interfaces.

As an example of the application of the methodology of Jones et al. (2009b), Fig. 1 shows the variation of log(resistivity) against shear wave velocity that would be experienced by a rock at 150 km below the Kaapvaal Craton if the only parameter varied was temperature. The lherzolitic composition is well known from the kimberlite studies of the craton.

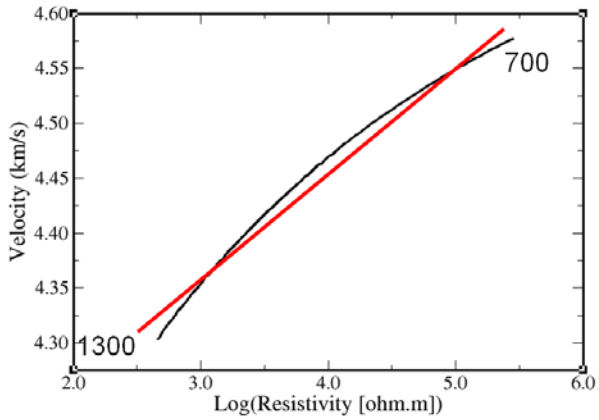

Figure 1. Black line: Variation of Log(resistivity) against shear wave velocity as a function of temperature from 700 °C to 1300 °C for a rock at a pressure of 4.63 GPa with a composition of Ol=65.5%, Opx=26.9%, Cpx=6.1% and Gn=1.3% and for a Mg# = 91.0 (assumed to be the same for all minerals). Red line: Best-fitting linear regression to black line.

The numerical data (black line, Fig. 1) can be fit to a linear regression (red line, Fig. 1), where

$$Vs_{150} = 4.2 + 0.096*\log_{10}(\rho_{150}\ [\Omega.m]) \quad [km/s].$$

A linear regression describes well variations around the centre of the curve, but poorly generally. The curve can be fit almost perfectly with a quadratic regression, resulting in the following:

$$Vs_{150} = 3.94 + 0.23*\log_{10}(\rho_{150}) - 0.017*(\log_{10}(\rho_{150}))^2.$$

NATURAL LABORATORY: S. AFRICA

In southern Africa, as a consequence of the world's largest-ever teleseismic study (Southern African Seismic Experiment, www.ciw.edu/mantle/kaapvaal/, SASE) followed by the world's largest-ever land-based MT project (Southern African MT Experiment, SAMTEX), the physical properties and geometries of Archean and Proterozoic lithosphere are becoming well-known. Coverage of the southern part of the continent by SASE and SAMTEX is shown in Fig. 2.

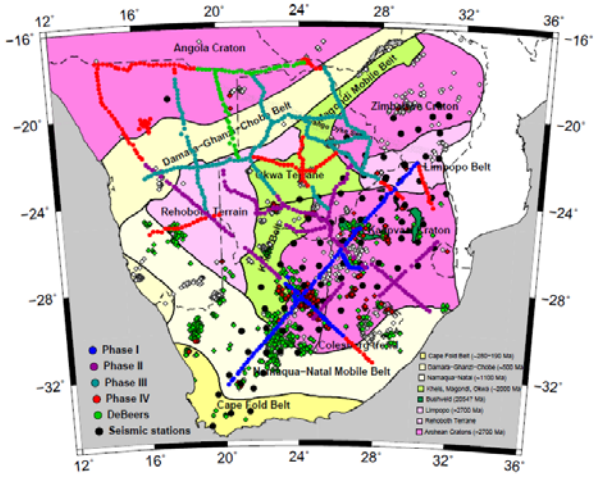

Figure 2. Coverage by SASE (black dots) and SAMTEX (coloured dots) in southern Africa, on a tectonic map (courtesy of Sue Webb). Kimberlite localities shown as diamonds: Red: known to be diamondiferous. Green: known to be non-diamondiferous. White: unknown (to us).

Southern Africa provides an excellent natural laboratory for testing theories about geophysical and geochemical relationships, given the extensive geophysical information from SASE and SAMTEX and the petrological information of the mantle lithosphere. The latter comes from analyses of xenoliths from virtually throughout the whole lithospheric depth extent and from much of the region due to kimberlite eruptions (diamonds in Fig. 2).

Qualitative comparisons between seismic models, both shear wave velocity model and shear and compressional body wave models, and the MT images already provided strong support for a correlation between fast and resistive areas and slow and conductive ones. These are shown in Figs. 7, 8 and 9 in Jones et al. (2009d). Herein we quantify the relationship between Vs and log(ρ) to test if the quadratic form suggested from considering laboratory observations is upheld.

Seismic shear wave velocity model at 100 km

A new seismic shear wave velocity model for Africa

was recently determined by Fishwick (unpubl.). The model is derived from tomographic inversion of surface wave dispersion curves from stations across Africa, including SASE, using a two-step approach described in Fishwick et al. (2005). In the first step, 1-D path-averaged models are fit to the fundamental and first four higher modes of the dispersion curve in the period range 50-120 s using the Debayle (1999) method. In the second step series of depth slices calculated using path average velocities with tomographic inversion code of Yoshizawa and Kennet (2002) using B-spline parameterisation and norm damping for regularisation. First, 8° knot point splines are fit to determine the large-scale structure, then smaller spacing (1.5°) knot points are used for detailed structure.

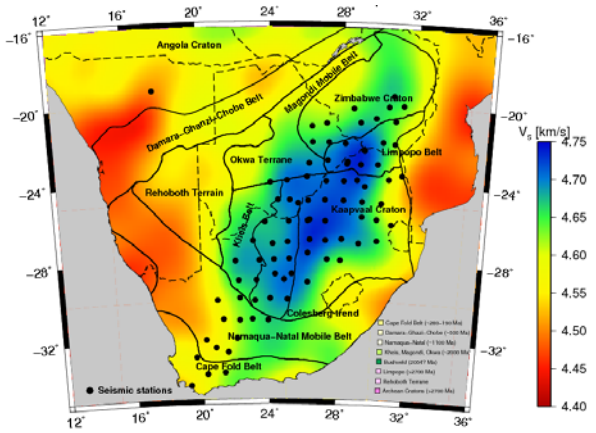

Figure 3: Shear wave velocity model at 100 km beneath Southern Africa from Fishwick (unpubl.)

The 100 km depth slice from Fishwick's latest model is shown in Fig. 3. A depth of 100 km is chosen as the resolution kernel is reasonably sharp, averaging information from below the base of the crust down to above the graphite-diamond stability field at about 150 km for the Kaapvaal Craton (Kennedy and Kennedy, 1976).

Electrical resistivity image at 100 km

The electrical resistivity at 100 km is determined using the approximate technique described in Jones et al. (2009d), and is shown in Fig. 4. The method involves determining the maximum "Niblett-Bostick" resistivity at a particular "Niblett-Bostick" depth below a station, then spatially smoothing to remove local static shift effects. A depth of 100 km is chosen as the attenuating effects of any crustal conducting layers will be reduced and the derived resistivity will have attained close to the correct resistivity (see Jones, 1999a, Fig. 3).

STATISTICAL COMPARISON

The cross-plot between the $\log_{10}$(NB resistivity [Ω.m]) derived beneath each MT station and the shear wave velocity [km/s] of the nearest node in the seismic model is shown in Fig. 5. The expected relationship from the mineral physics arguments is shown as a red line, whereas the best-fitting quadratic equation to the data is shown in the blue line.

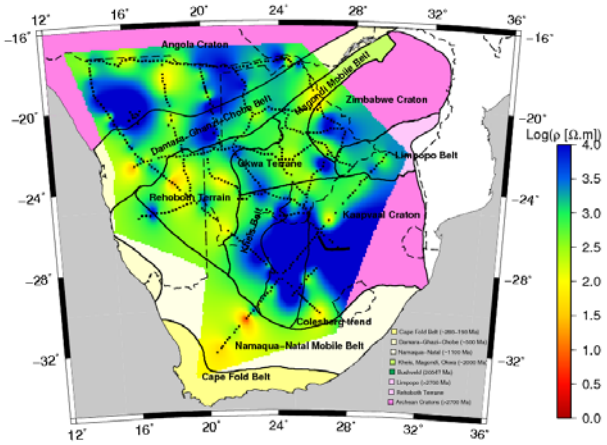

Figure 4: Resistivity image at 100 km beneath Southern Africa after Jones et al. (2009c).

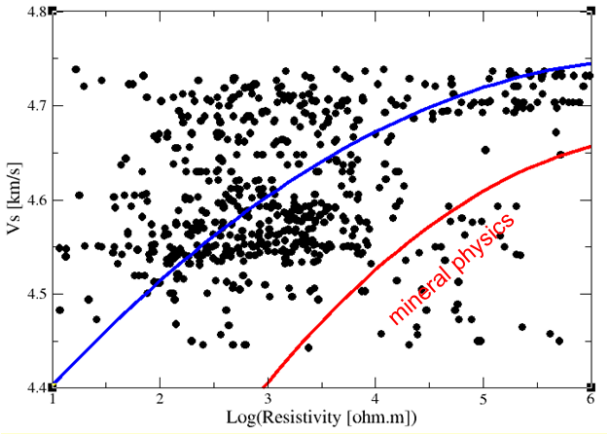

Figure 5: Log_{10}(NB Resistivity) vs. Shear wave velocity cross-plot of the data contoured in Figs. 3 and 4. The **red line** is the expectation from mineral physics arguments (Jones et al., 2009a), and the **blue line** is best-fitting quadratic equation.

The prediction of Vs from $\log_{10}(\rho_{NB})$ is given by:
$\mathbf{Vs_{100} = 4.27 + 0.14*\log_{10}(\rho_{100}) - 0.011*(\log_{10}(\rho_{100}))^2}$.

How well does this prediction describe the observations? This is tested through applying the quadratic equation above, deriving estimated shear wave velocities, smoothing the resulting predictions with a 1.5° median filter to reproduce the spatial smoothing applied to the seismic velocity model, and subtracting the predicted velocity model from the actual velocity model. The difference plot is shown in Fig. 6 below. Essentially, if the velocity model is accurate to a level of ±0.05 km/s, then for approx. 75% of Southern Africa the quadratic description holds to within experimental error. If the accuracy of the model is somewhat less precise, at a level of ±0.10 km/s, then

for 95% of Southern Africa the prediction holds.

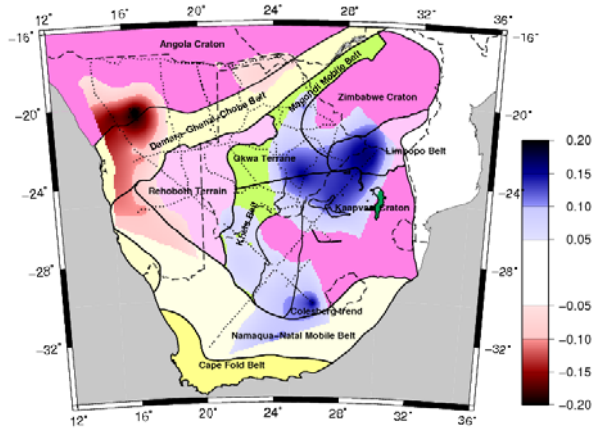

Figure 6: Difference between actual veolocity model (Fig. 3) and velocity model predicted from the resistivity image using the quadratic relationship above. Where the difference is less than ±0.05 km/s the image is transparent.

Two areas do not fit the parametric description. One is in NE South Africa and SW Zimbabwe, and is related to reduced resistivity in the mantle from Bushveld processes that do not correspondingly reduce seismic velocity in the quadratic manner expressed above. The second is in NW Namibia, where the velocities are too low compared to the resistivities. This is harder to explain. However, that for much of Southern Africa there is a statistical quadratic relationship between seismic velocity and electrical resistivity means that the velocity variation is driven primarily by temperature variation, not compositional variation.

CONCLUSIONS

We have demonstrated that for much of Southern Africa there is a systematic quadratic relationship between seismic shear wave velocity and estimated electrical resistivity at a depth of 100 km. This is quite an astounding result, and implies that lateral velocity variation is primarily temperature-driven not compositionally-driven.

REFERENCES

Bleeker, W., 2003. The late Archean record: a puzzle in ca. 35 pieces. Lithos, 71(2-4): 99-134.

Davies, G.F., 1992. On the emergence of plate tectonics. Geology, 20: 963–966.

Davis, W.J., Jones, A.G., Bleeker, W. and Grutter, H., 2003. Lithosphere development in the Slave craton: a linked crustal and mantle perspective. Lithos, 71(2-4): 575-589.

de Wit , M.J., 1998. On Archean granites, greenstones, cratons and tectonics: Does the evidence demand a verdict? Precambrian Research, 91: 181-226.

Debayle, E., 1999. SV-wave azimuthal anisotropy in the Australian upper mantle: preliminary results from automated Rayleigh waveform inversion. Geophysical Journal International, 137(3): 747-754.

Fishwick, S., Kennett, B.L.N. and Reading, A.M., 2005. Contrasts in lithospheric structure within the Australian Craton - insights from surface wave tomography. Earth and Planetary Science Letters, 231(3-4): 163-176.

Hamilton, W.B., 1998. Archean magmatism and deformation were not products of plate tectonics. Precambrian Research, 91: 143-179.

Hill, R., 1952. Elastic properties of reinforced solids: some theoretical principles. Proceedings of the Physics Society of London Series A, 65: 349–354.

Hoffman, P.F., 2006. Evidence from ophiolites, blueschists, and ultrahigh-pressure metamorphic terranes that the modern episode of subduction tectonics began in Neoproterozoic time: Comment. Geology, 34: e105.

Jones, A.G., 1998. Waves of the future: Superior inferences from collocated seismic and electromagnetic experiments. Tectonophysics, 286(1-4): 273-298.

Jones, A.G., 1999a. Imaging the continental upper mantle using electromagnetic methods. Lithos, 48(1-4): 57-80.

Jones, A.G., 1999b. Information about the continental mantle from deep electromagnetic studies, Short Course on Geophysical and Geochemical Imaging of Canada's Upper Mantle, Yellowknife, NWT, Canada.

Jones, A.G., Evans, R.L. and Eaton, D.W., 2009a. Velocity-conductivity relationships for mantle mineral assemblages in Archean cratonic lithosphere based on a review of laboratory data and application of extremal bound theory. Lithos, 109: 131-143.

Jones, A.G., Evans, R.L. and Eaton, D.W., 2009b. Velocity-conductivity relationships for mantle mineral assemblages in Archean cratonic lithosphere based on a review of laboratory data and Hashin-Shtrikman extremal bounds. Lithos, 109(1-2): 131-143.

Jones, A.G. et al., 2009c. The SAMTEX experiment: Overview and Preliminary Results, 2009 SAGA Biennial Technical Meeting & Exhibition, Swaziland.

Jones, A.G. et al., 2009d. Area selection for diamonds using magnetotellurics: Examples from southern Africa. Lithos, 112: 83-92.

Kennedy, C.S. and Kennedy, G.C., 1976. Equilibrium boundary between graphite and diamond. Journal of Geophysical Research - Solid Earth, 81(14): 2467-2470.

Muller, M.R. et al., 2009. Lithospheric structure, evolution and diamond prospectivity of the Rehoboth Terrane and western Kaapvaal Craton, southern Africa: Constraints from broadband magnetotellurics. Lithos, 112: 93-105.

Reuss, A., 1929. Berechung der Fliessgrenze von Mischkristallen auf Grund der Plastizitätsbedingung für Einkristalle. Zeitschrift für Angewandte Mathematik und Mechanik, 9: 49–58.

Stern, R.J., 2005. Evidence from ophiolites, blueschists, and ultrahigh-pressure metamorphic terranes that the modern episode of subduction tectonics began in Neoproterozoic time. Geology, 33: 557-560.

Stern, R.J., 2006. Evidence from ophiolites, blueschists, and ultrahigh-pressure metamorphic terranes that the modern episode of subduction tectonics began in Neoproterozoic time: Reply. Geology, 34: e105-e106.

Stern, R.J., 2007. When and how did plate tectonics begin? Theoretical and empirical considerations. Chinese Science Bulletin, 52(5): 578-591.

van Kranendonk, M.J. (Editor), 2003. Archean tectonics in 2001: an Earth odyssey. Precambrian Research, 1-3.

Voigt, W., 1928. Lehrbuch der Kristallphysik. Teubner, Leipzig.

Yoshino, T., 2010. Laboratory electrical conductivity measurement of mantle minerals. Surveys in Geophysics, 31(2): 163-206.

Yoshizawa, K. and Kennett, B.L.N., 2002. Non-linear waveform inversion for surface waves with a neighbourhood algorithm - application to multimode dispersion measurements. Geophysical Journal International, 149(1): 118-133.